Title: Rejuvenating Senescent Cells and Organisms with Only Ultrasound

Authors: Sanjay Kumar[1], Rosario Maroto[1], Simon Powell[1], Felix Margadant[2], Brandon Blair[1], Blake B. Rasmussen[1], Michael Sheetz[1*]

Affiliations:

[1]Biochemistry and Molecular Biology, University of Texas Medical Branch; 301 University Blvd., Galveston, Texas, 77555.
[2]Visiting Scientist, Biochemistry and Molecular Biology, University of Texas Medical Branch; 301 University Blvd., Galveston, Texas, 77555.

*Corresponding author. misheetz@utmb.edu

Abstract:
Accumulation of senescent cells in tissue and organs leads to aging abnormalities. Rejuvenating senescent cells provides a strategy to ameliorate aging. We report here that low frequency ultrasound (LFU) rejuvenates senescent cells causing growth and loss of senescence markers. With fibroblasts and mesenchymal stem cells, LFU can enable increased cell expansion without altering phenotype. At a subcellular level, LFU causes mitochondrial fission and loss of lysosome staining that is enhanced by rapamycin or Rho kinase inhibition and blocked by Sirtuin1 inhibition, consistent with the hypothesis that LFU activates autophagy. In vivo, older mice are rejuvenated by LFU as measured by increased physical performance and decreased levels of senescent cells in kidney and pancreas measured by three markers. Thus, we suggest that LFU alone increases aged cell and whole animal performance.

One-Sentence Summary: Low frequency ultrasound alone rejuvenates senescent cells and aged mice by activating autophagy.

Introduction:

Cell senescence is one of the hallmarks of the aging process [1, 2]. Transplantation of senescent cells into young mice causes physical deterioration and age related pathologies [3], whereas depletion of these cells from aged mice slows age-related pathologies and enhances life

span [4-12]. This indicates that cellular senesence is one of the drivers of the aging process and removing senescent cells is critical for improving performance in aged organisms. Senescence is characterized by a state of permanent cell cycle arrest where cells are metabolically active but stop dividing [13]. In 1961, Hayflick reported that primary cells in culture stopped growing after a certain number of divisions, because they became senescent [14]. The understanding of senescence is important because the accumulation of senescent cells in most tissues causes age-related pathologies [15-17], including in lung, adipose tissue, aorta, pancreas, and osteoarthritic joints [10]. There are potentially many benefits from decreasing the fraction of senescent cells in tissues.

The senescence process has general physiological significance since it prevents the propagation of damaged cells, suppresses tumor progression, helps in early development [11], wound healing [12].and in tissue repair processes [13]. Despite the beneficial roles of senescent cells, there are many age associated maladies [14]; and senescent cells secrete many pro-inflammatory molecules, growth factors, chemokines, extracellular matrices, proteases and cytokines, collectively known as senescence associated secretary phenotype (SASP) [15]. An increase in the level of SASP catalyzes many age-related problems [16]. Therefore, targeted elimination of senescent cells can potentially improve age-associated pathologies including osteoarthritis [2], diabetes [17], osteoporosis, neurodegenerative disease [18], and overall lifespan [3]. Rejuvenation of senescent cells is seen as an unmet need to develop rejuvenating or activating strategies in aging organisms.

Autophagy inhibition and mitochondrial dysfunction are hallmarks of aging and cellular senescence[1]. Dynamic changes in mitochondrial fusion and fission are essential for healthy mitochondrial function and increased fusion contributes to cell senescence [19]. There is evidence of decreased senescence with exercise [20] that may be related to unknown processes that increase mitochondrial fission [21]. Although changes in lysosome and mitochondrial functions may be related, there is significant evidence that inhibition of lysosomal autophagy is a driver for aging [22].

Pharmacological elimination of senescent cells by Senolytics is one strategy to diminish effects of aging by apoptosis [23, 24] that has gone to clinical trials [41]. However, there is currently no approved senolytic treatment for humans [25].

Ultrasound treatment can reverse cell senescence.

We report here that ultrasound treatment can rejuvenate senescent cells. Ultrasound produces short duration pressure waves in cells that create mechanical stresses. These conditions are safe for normal tissues and do not adversely influence functions of normal cells [41]. We report here that in cases of chemically-induced or replicative senescent cells, low frequency ultrasound (LFU) treatment can restore normal behavior. Cells grow, no longer secrete SASP, their size decreases, and their mitochondria decrease in length. Surprisingly, we find that normal cells treated with LFU secrete factors that activate senescent cell growth. Further, aged mice are rejuvenated by LFU and have fewer senescent cells in their organs. Thus, it seems that LFU alone can reverse the negative effects of cell senescence.

RESULTS

To test the generality of LFU treatments for reversing cell senescence, we induced cell senescence with four compounds: doxorubicin, hydrogen peroxide, sodium butyrate and bleomycin sulfate. Senescence was characterized by a decreased growth rate, increased β-galactosidase activity, increased cell size, and secretion of pro-inflammatory factors called SASP [15]. All four criteria were met with each type of senescent cells (Figure 1A) in that cell growth was effectively blocked (Figure 1B), cell size increased (Figure 1C and 1D) [27], cells secreted SASP [15] (Figure 1E) and β-galactosidase activity increase (Figure 1F and 1G). Thus, by all criteria, the four different types of treated cells were indeed senescent.

LFU Rejuvenates Senescent Cells and Causes Normal Cell Secretion of Growth Factors for Senescent Cells

To determine if mechanical activity could reverse some of the phenotypes of the senescent cells, we treated them with LFU at intermediate power levels. After irradiation for twenty minutes, the cells were passaged every 48 hours (Figure 2A). Cells grew after LFU treatment for 12-15 days without significantly diminishing in growth rate (Figure 2B). LFU treatment caused cell size to decrease to that of normal cells over 8-10 days (Figure 2C). LFU treated cells show reduced level of cell cycle inhibitor p21 (Figure 2D and 2E). All four senescent cell lines grew after ultrasound irradiation, decreased in size, and decreased in p21 expression. LFU treatment blocked the secretion of SASP (Figure S1A-S1D). The reversal was partial in all cases but provided a promising possibility that ultrasound could rejuvenate senescent cells.

Many studies have shown that physical exercise delays tissue and brain aging [20, 28]. To test the possibility that LFU could benefit senescent cells through their normal neighbors, we treated normal cells with LFU over a period of three days (1 h per day) and then collected the supernatant (USS) for culturing senescent Vero cells (Figure S1E). Surprisingly, USS activated growth (Figure S1F and S1G) and decreased spread area of senescent cells (Figure S1H). Thus, LFU treatment stimulated secretion of factors from normal cells that caused growth of senescent cells.

LFU Rejuvenation of Senescent Cells with Mitochondrial Fission and Autophagy Activation

Since senescence was associated with an increase in mitochondrial fusion [29], we followed the changes in mitochondrial length during senescence and the reversal of senescence by LFU. Further, we also examined Lysosome and microtubule morphologies since they have also been known to change during senescence compared to normal cells (Figure 3A). There was a significant increase in mitochondrial length and in the number of lysosomes in the senescent cells [19, 29]. After LFU treatment, the mitochondria were fragmented, and their average length decreased

(Figure 3A and 3C). Further, lysosome staining decreased relative to mitochondrial staining (Figure 3B). However, microtubule staining showed that LFU treatment had no apparent effect on microtubule distribution or length (Figure S2). Thus, there was a significant effect of LFU on mitochondrial and lysosome morphology that belied a major change in the organization of those organelles that occurred without altering microtubule morphology.

If LFU was acting by activating autophagy as suggested in our working model (Figure 3D), then rapamycin, which is known to activate autophagy by inhibiting mTORC1, should be synergistic with ultrasound [22]. As predicted, addition of rapamycin increased rejuvenation of LFU-treated cells (Figure S3E). In yeast, the process of senescence was associated with decreased activity of the deacetylase ser1; and sirtuin1, a mammalian analog, was linked to senescence [30]. When we inhibited sirtuin1 during LFU treatment of senescent cells, we discovered that rejuvenation of senescence was blocked (Figure S3A to S3D) .

Previous studies from our laboratory reported that a different LFU treatment caused apoptosis of tumor cells but not normal cells [31]. In that case, LFU-dependent tumor cell apoptosis increased after microtubule depolymerization by nocodazole and the Rho kinase inhibitor (Y-27632) blocked apoptosis. Depolymerization of microtubules increases Rho kinase activity and myosin contractility [32] whereas the Rho kinase inhibitor decreases contractility. In the case of LFU induced senescent cell rejuvenation, addition of Y-27632 increased rejuvenation while microtubule depolymerization had no effect (Figure S3F). Thus, the reversal of senescence by LFU was different from the activation of tumor cell apoptosis by involving other cytoskeletal elements.

Expansion of Replicative Senescent Cells by LFU

Because replicative senescence presumably was a common property of normal cells that limited growth [8], we tested whether LFU could extend the growth potential of normal cells. After

15 passages human foreskin fibroblasts (HFFs) decreased in growth rate, increased in average cell size, and exhibited increased β-galactosidase activity. However, after LFU treatment with every other passage, for passages 15-24, HFF cells behaved like normal cells and continued to grow without a change in growth rate for at least 24 passages (Figure 4A). This made it possible to grow >7,500 (2^{13}) fold more HFF cells than without LFU, while morphology was normal (Figure 4B) without senescence markers (Figure 4C). When P24 LFU cells were cultured on soft matrices, they ceased to grow (Figure S4), showing rigidity-dependent growth. Similarly, we expanded mesenchymal stem cells (MSCs) with LFU beyond the normal replicative limit (Figure 4D). Upon treatment with differentiation medium, the LFU expanded MSCs differentiated normally into adipocytes or osteocytes, depending upon the medium (Figure 4E). Thus, LFU induced growth of replicative senescent cells without causing transformation or apparent changes in cell phenotype.

LFU Improves Aged Mouse Performance

As with many older organisms, older mice have decreased physical function in performance tests. We tested the performance of 22–25-month-old mice (C57BL/6) with the comprehensive functional assessment battery (CFAB) [33], which included four tests: treadmill, inverted cling, grip strength, and rotarod tests. Animals were tested before and after treatment over three months with LFU treatment for 30 min. every third day in the first and third months while the second month was without treatment (Figure 5A). There were 6 groups of 4 male and 4 female mice that were 1) untreated, 2) treated with LFU, 3) treated with exercise (20 min on treadmill for 12 times per month), 4) treated with LFU and exercise, 5) treated with rapamycin, and (6) treated with rapamycin and LFU. The LFU treated animals showed improved performance in most cases except for the grip and rotarod tests (data not shown). Statistically significant improvements were consistently observed with the LFU alone group, the rapamycin plus LFU and the exercise plus LFU groups (Figure 5B and 5D). There was a decrease in the performance after one month off in

the ultrasound treated groups; however, the second month of treatment restored significant improvement in the LFU and rapamycin plus LFU groups (Figure 5C and 5E). Thus, LFU treatment alone and in synergy with rapamycin or exercise significantly improved physical performance of aged (22 to 25 mo.) animals in tests of performance.

Senescent Cell Density in Pancreas and Kidney Is Reduced Several Fold by LFU

To determine if LFU reversed senescence in the pancreas and kidney of the aged animals, we euthanized animals, removed organs, fixed, and sectioned the organs. In the case of animals that were treated with LFU for two months (10 treatments in the first and third months), animals were sacrificed 5 days after the last LFU treatment. Sections of the pancreas and kidney were stained for the senescent cell markers, p16 and p21 (Figure S5A and S5B). There was a remarkably high fraction of fluorescent cells in the pancreas of sham animals (about 60% of the cells stained with the anti-p21 antibody, 20% with the anti-p16 antibody (Figure S5D), which was similar to previous observations [10]. However, after LFU treatment, the staining for both p21 and p16 was notably decreased to 20% and 5% respectively (Figure S5D and S5F). In the kidney, there was a high fraction of fluorescent cells (32% stained for p21 and 38% stained for p16), which decreased to 15 and 17%, respectively (Figure S5C and S5E). Thus, the LFU treatment significantly decreased the fraction of senescent cells in the pancreas and kidney as measured by p21 and p16 staining.

In a second experiment mice were treated with LFU (either daily, every other day, or every third day with 1X LFU and daily with 1.3X or 2X power levels) (Figure S6A). After two weeks of treatment, performance improved with all LFU conditions but was statistically significant with 1.3X power (Figure S6B and S6D). A second treatment of two weeks increased performance relative to the sham animals particularly in the inverted cling test (Figure S6C and S6E). We then sacrificed mice and dissected/fixed organs. After sectioning and staining for β-galactosidase

(Figure 6A), there was ~70% of the pancreas area and ~70% of the kidney showing significant staining in the sham animals (Figure 6B and 6C). Treated animals showed decreased staining to 10-30% depending upon the treatment (Figure 6D and 6E). The variation in the levels of staining in the treated animals did not show a pattern that fitted with the changes in performance levels (Figure S6) and we suggest that this was due to biological variance. Overall, LFU treated animals had very significant decreases in the fraction of senescent cells in the pancreas and kidney as determined by 3 different senescence markers, which correlated with improved performance.

Discussion

These studies show that senescent cells can be mechanically rejuvenated without transfection or other biochemical manipulation by LFU. The ultrasound pressure waves restore normal behavior to senescent cells irrespective of whether senescence was induced by chemical treatment or by repeated replication. The features of senescent cells are all reversed by ultrasound treatment, including the increase in β-galactosidase activity, increase in cell size, secretion of SASP and inhibition of growth. Restoration of normal behavior correlates with a decrease in mitochondrial length and a decrease in lysosomal volume but microtubule morphology was not affected. Surprisingly, ultrasound treatment of normal cells causes secretion of growth stimulating factors that partially restore normal behavior in senescent cells. Because replicative senescent cells are restored to a normal phenotype, they can be cultured for long periods to produce increased numbers of cells without apparent alteration in phenotype.

Mechanical effects on cell behavior have been known for a long time. However, recently it has become clear that controlled mechanical perturbations reproducibly alter cell functions and phenotypic behaviors. Tumor cells are mechanosensitive since either stretching, fluid shear or ultrasound can cause apoptosis in vitro [35]. In addition, exercise appears to inhibit tumor growth in

vivo [36]. Similarly, in the studies presented here, the normal cell state was not altered by the mechanical treatments whereas senescent cells were rejuvenated.

There is evidence of a correlation between exercise and a reversal of senescent cells in older animals and humans [20]. Individual cells have not been followed and it is not clear if exercise reverses senescence or is a Senolytic. In these studies, it is clear that ultrasound pressure waves alone can reverse senescent cell to normal cell behavior, i.e. rejuvenate them, without causing cell death. The ultrasound and exercise effects are synergistic with and both will cause cell deformations. We suggest that both exercise and LFU will rejuvenate cells in situ without apoptosis and will increase the performance of aged animals. The selective lysis of senescent cells is an alternative approach to senescence and it has been shown to improve performance of older mice [4, 37]. The critical issue for improving the performance of aged mice is that the number of senescent cells in the animal decreases, whether through senolytics, exercise or LFU.

The senescent cell state has been extensively studied but the molecular bases for the changes are not fully understood. There are major roles for changes in autophagy and mitochondria in senescence [22, 38]. Accordingly, most models of the senescence process postulate major roles for changes in autophagy and mitochondria function with changes in the communication between lysosomes, mitochondria and other cellular organelles. Consistent with these hypotheses (modeled in Figure 3D), we find that LFU causes mitochondrial fission and the loss of lysosomes. The subcellular effects of ultrasound appear to be mediated by mechanically dependent mitochondria-ER-lysosome interactions that activate lysosomal autophagy and mitochondrial changes that are manifested in changes in length. Thus, we suggest that LFU induced distortion acts on organized elements of the cytoplasm like exercise to reverse changes induced by senescence. At a molecular level, senescence is associated with active mTORC1 binding to lysosomes thereby inactivating autophagy [39]. Rapamycin inhibition of mTORC1 is synergistic with LFU-induced rejuvenation

and rejuvenation correlates with activation of autophagy as evidenced by a decrease in lysosomal staining (Figure 3B). In the case of Sirtuin 1, loss of activity is associated with an increase in senescence, which fits with the need for Sirtuin 1 activity in rejuvenation (Figure S3) [30]. Much more research is needed to understand how LFU pressure waves could inhibit mTORC1 and activate Sirtuin1 enzyme function.

Cellular changes with senescence are extensive and involve not only changes in organelle architecture but also in the secretory pathways that produce SASP. The surprising finding of growth stimulatory factors that are secreted by normal cells upon LFU stimulation indicates that LFU mechanical effects may be part of a larger network of functions that support systemic responses to physical exercise. For example, exercise stimulates the secretion of myokines that benefit brain function and quality of life [40]. We suggest that the effects of LFU mimic many of the effects of exercise at a cellular level with the added benefit that LFU can penetrate the human body to reach internal organs.

The growth activation of replicative senescent cells by non-invasive LFU has important implications for the in vitro expansion of normal cells to aid in autologous repair procedures. Much more research is needed to understand the extent of the expansion that is possible. However, we find that expansion does not involve apparent damage to the cells or modification of their phenotype. This indicates that the ultrasound reversal of senescence can have major benefits in enabling the continued growth of normal cells beyond current limits. Because ultrasound has been approved for human exposure at power levels ten to hundred-fold higher than the levels used in this study, we suggest that it is practical to develop ultrasound-based therapies that could inhibit the increase in the fraction of senescent cells in tissues with aging and thereby inhibit the onset of many age-related maladies. Most importantly, these results show that mechanical treatments can

replace biochemical treatments to produce desired reversal of senescence and they are consistent with known effects of exercise on senescence and quality of life with aging.

Acknowledgments:

We want to acknowledge the experimental help of Adam Baker. We greatly appreciated the advice in editing this manuscript provided by Linda Kenney. Dr. Felix Margadant and Simon Powell provided support in fabrication of ultrasound devices and their maintenance.

Funding:

UTMB Biochemistry and Molecular Biology Department startup funds (MS)

CPRIT Foundation grant RR180025 (MS)

Welch Foundation professorship (MS)

Claude D. Pepper Older Americans Independence Center Pilot Project Grant (MS and BR)

NSF grant 1933321 (Co-I MS)

Author contributions:

Conceptualization: MS, SK, BR

Methodology: SK, RM, SP, FM

Writing: MS, SK, BR,

Experimentation: SK, RM, BB

Competing interests: Authors (MS, SK, FM, and RM) are co-authors of patents related to these studies.

Data and materials availability: All data are available in the main text or the supplementary materials.

REFERENCES

1. J. M. van Deursen, The role of senescent cells in ageing. *Nature* **509**, 439-446 (2014).
2. M. Xu *et al.*, Transplanted Senescent Cells Induce an Osteoarthritis-Like Condition in Mice. *J Gerontol A Biol Sci Med Sci* **72**, 780-785 (2017).
3. M. Xu *et al.*, Senolytics improve physical function and increase lifespan in old age. *Nat Med* **24**, 1246-1256 (2018).
4. J. Chang *et al.*, Clearance of senescent cells by ABT263 rejuvenates aged hematopoietic stem cells in mice. *Nat Med* **22**, 78-83 (2016).
5. W. Peilin *et al.*, Directed elimination of senescent cells attenuates development of osteoarthritis by inhibition of c-IAP and XIAP. *Biochim Biophys Acta Mol Basis Dis* **1865**, 2618-2632 (2019).
6. G. Watts, Leonard Hayflick and the limits of ageing. *Lancet* **377**, 2075 (2011).

7. B. G. Childs, M. Durik, D. J. Baker, J. M. van Deursen, Cellular senescence in aging and age-related disease: from mechanisms to therapy. *Nat Med* **21**, 1424-1435 (2015).
8. L. Hayflick, P. S. Moorhead, The serial cultivation of human diploid cell strains. *Exp Cell Res* **25**, 585-621 (1961).
9. S. He, N. E. Sharpless, Senescence in Health and Disease. *Cell* **169**, 1000-1011 (2017).
10. B. Molla *et al.*, Two different pathogenic mechanisms, dying-back axonal neuropathy and pancreatic senescence, are present in the YG8R mouse model of Friedreich's ataxia. *Dis Model Mech* **9**, 647-657 (2016).
11. M. Storer *et al.*, Senescence is a developmental mechanism that contributes to embryonic growth and patterning. *Cell* **155**, 1119-1130 (2013).
12. M. Demaria *et al.*, An essential role for senescent cells in optimal wound healing through secretion of PDGF-AA. *Dev Cell* **31**, 722-733 (2014).
13. D. Munoz-Espin, M. Serrano, Cellular senescence: from physiology to pathology. *Nat Rev Mol Cell Biol* **15**, 482-496 (2014).
14. B. G. Childs *et al.*, Senescent cells: an emerging target for diseases of ageing. *Nat Rev Drug Discov* **16**, 718-735 (2017).
15. T. Tchkonia, Y. Zhu, J. van Deursen, J. Campisi, J. L. Kirkland, Cellular senescence and the senescent secretory phenotype: therapeutic opportunities. *J Clin Invest* **123**, 966-972 (2013).
16. J. P. Coppe *et al.*, Senescence-associated secretory phenotypes reveal cell-nonautonomous functions of oncogenic RAS and the p53 tumor suppressor. *PLoS Biol* **6**, 2853-2868 (2008).
17. P. J. Thompson *et al.*, Targeted Elimination of Senescent Beta Cells Prevents Type 1 Diabetes. *Cell Metab* **29**, 1045-1060 e1010 (2019).
18. J. Penney, L. H. Tsai, Elimination of senescent cells prevents neurodegeneration in mice. *Nature* **562**, 503-504 (2018).
19. J. Chapman, E. Fielder, J. F. Passos, Mitochondrial dysfunction and cell senescence: deciphering a complex relationship. *FEBS Lett* **593**, 1566-1579 (2019).
20. D. A. Englund *et al.*, Exercise reduces circulating biomarkers of cellular senescence in humans. *Aging Cell* **20**, (2021).
21. S. C. J. Helle *et al.*, Mechanical force induces mitochondrial fission. *Elife* **6**, (2017).
22. J. M. Carosi, C. Fourrier, J. Bensalem, T. J. Sargeant, The mTOR-lysosome axis at the centre of ageing. *FEBS Open Bio* **12**, 739-757 (2022).
23. Y. Zhu *et al.*, The Achilles' heel of senescent cells: from transcriptome to senolytic drugs. *Aging Cell* **14**, 644-658 (2015).
24. M. J. Yousefzadeh *et al.*, Fisetin is a senotherapeutic that extends health and lifespan. *EBioMedicine* **36**, 18-28 (2018).
25. J. L. Kirkland, T. Tchkonia, Cellular Senescence: A Translational Perspective. *EBioMedicine* **21**, 21-28 (2017).
26. F. Ahmadi, I. V. McLoughlin, S. Chauhan, G. ter-Haar, Bio-effects and safety of low-intensity, low-frequency ultrasonic exposure. *Prog Biophys Mol Biol* **108**, 119-138 (2012).
27. R. A. Veitia, DNA Content, Cell Size, and Cell Senescence. *Trends Biochem Sci* **44**, 645-647 (2019).
28. X. K. Chen *et al.*, Is exercise a senolytic medicine? A systematic review. *Aging Cell* **20**, e13294 (2021).

29. S. Mai, M. Klinkenberg, G. Auburger, J. Bereiter-Hahn, M. Jendrach, Decreased expression of Drp1 and Fis1 mediates mitochondrial elongation in senescent cells and enhances resistance to oxidative stress through PINK1. *J Cell Sci* **123**, 917-926 (2010).
30. T. Liu *et al.*, SIRT1 reverses senescence via enhancing autophagy and attenuates oxidative stress-induced apoptosis through promoting p53 degradation. *Int J Biol Macromol* **117**, 225-234 (2018).
31. A. Singh *et al.*, Enhanced tumor cell killing by ultrasound after microtubule depolymerization. *Bioeng Transl Med* **6**, e10233 (2021).
32. K. Chitaley, R. C. Webb, Microtubule depolymerization facilitates contraction of vascular smooth muscle via increased activation of RhoA/Rho-kinase. *Med Hypotheses* **56**, 381-385 (2001).
33. T. G. Graber, R. Maroto, C. S. Fry, C. R. Brightwell, B. B. Rasmussen, Measuring Exercise Capacity and Physical Function in Adult and Older Mice. *J Gerontol A Biol Sci Med Sci* **76**, 819-824 (2021).
34. M. L. Idda *et al.*, Survey of senescent cell markers with age in human tissues. *Aging (Albany NY)* **12**, 4052-4066 (2020).
35. M. Sheetz, A Tale of Two States: Normal and Transformed, With and Without Rigidity Sensing. *Annu Rev Cell Dev Biol* **35**, 169-190 (2019).
36. H. Rundqvist *et al.*, Cytotoxic T-cells mediate exercise-induced reductions in tumor growth. *Elife* **9**, (2020).
37. J. N. Farr *et al.*, Targeting cellular senescence prevents age-related bone loss in mice. *Nat Med* **23**, 1072-1079 (2017).
38. Y. Xu, W. Wan, Acetylation in the regulation of autophagy. *Autophagy*, 1-9 (2022).
39. Z. Zi *et al.*, Quantitative phosphoproteomic analyses identify STK11IP as a lysosome-specific substrate of mTORC1 that regulates lysosomal acidification. *Nat Commun* **13**, 1760 (2022).
40. B. So, H. J. Kim, J. Kim, W. Song, Exercise-induced myokines in health and metabolic diseases. *Integr Med Res* **3**, 172-179 (2014).
41. J. L. Kirkland, T. Tchkonia, Y. Zhu, L. J. Niedernhofer, P. D. Robbins, The Clinical Potential of Senolytic Drugs. *J Am Geriatr Soc* **65**, 2297-2301 (2017).

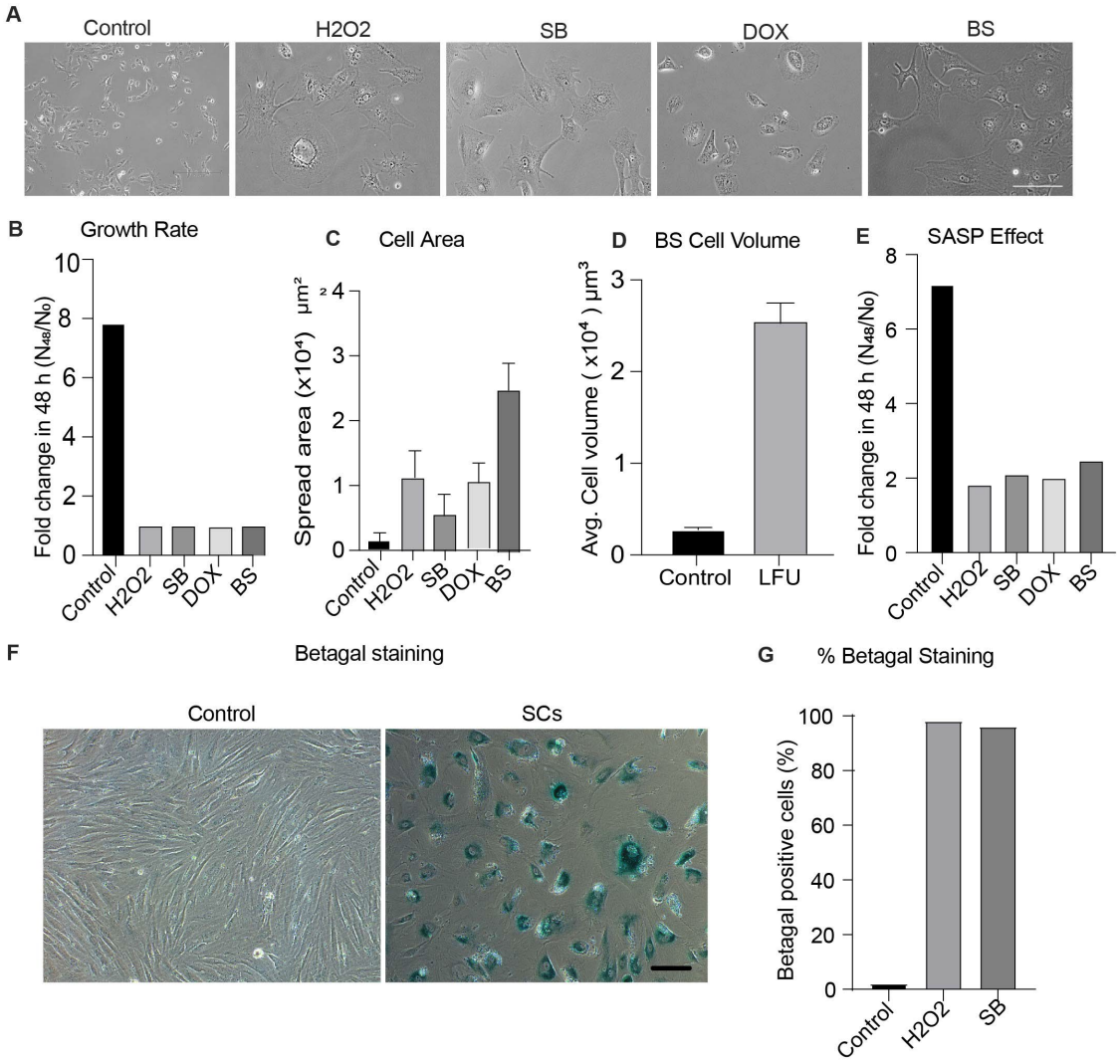

Figure 1 Characterization of Senescent Cells. (A) Brightfield images of senescent cells induced by H_2O_2, sodium butyrate (SB), Doxorubicin (Dox), and Bleomycin Sulphate (BS). Scale bar=300 µm. (B) Quantification of proliferation shows no senescent growth after a 48 h incubation. (C) Senescent cells become enlarged compared to the normal control cells. (D) Quantification of avg. cell volume of bleomycin sulfate treated cells compared to control cells. (E) Conditioned medium from senescent cells inhibits the growth of normal proliferating cells. (G) SA-b-galactosidase staining of control (proliferating) and BS treated senescent cells. Scale bar= 300 µm. (H) Level of b-galactosidase senescence marker in H_2O_2 and SB induced SCs. Scale bar= 300 µm. Data in (B)-(E) and (H) are mean ± SD. Minimum of 150 cells were analyzed for spread area and cell volume from n=2 experiments.

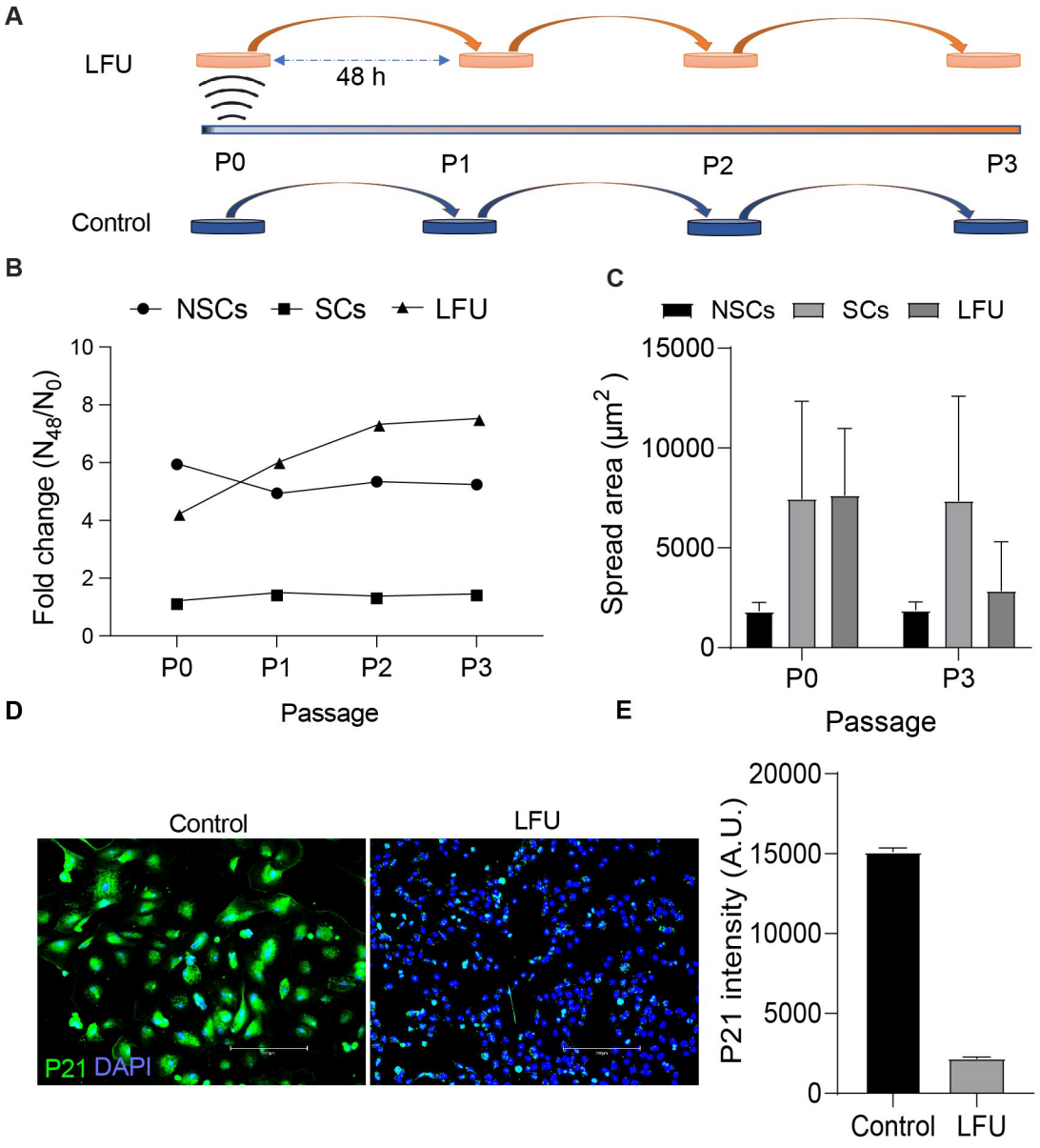

Figure 2 Ultrasound Reverses Cell Senescence. (A) Schematic illustration of senescence reversal experiment. SB treated Vero cells were treated with low frequency ultrasound (LFU) and passaged after every 48 h for 8-10 days. (B) Graph showing growth of normal control (NSC), BS senescent (SC) and LFU treated (LFU) senescent cells as fold change over 48 h for passage from P0 to P3 every 48 h. (C) Cell area of LFU treated senescent cells (LFU) is largely restored to normal by P3. (D) Representative anti-p21 immunofluorescence images of P3 control and LFU treated cells. Scale bar= 300 μm (E) Quantification of fluorescence intensity of p21 stained control and LFU treated P3 cells shown as mean ± SD, for >200 cells in each condition. All graphs were plotted by mean ± SD. Minimally 200 cells were analyzed in each condition.

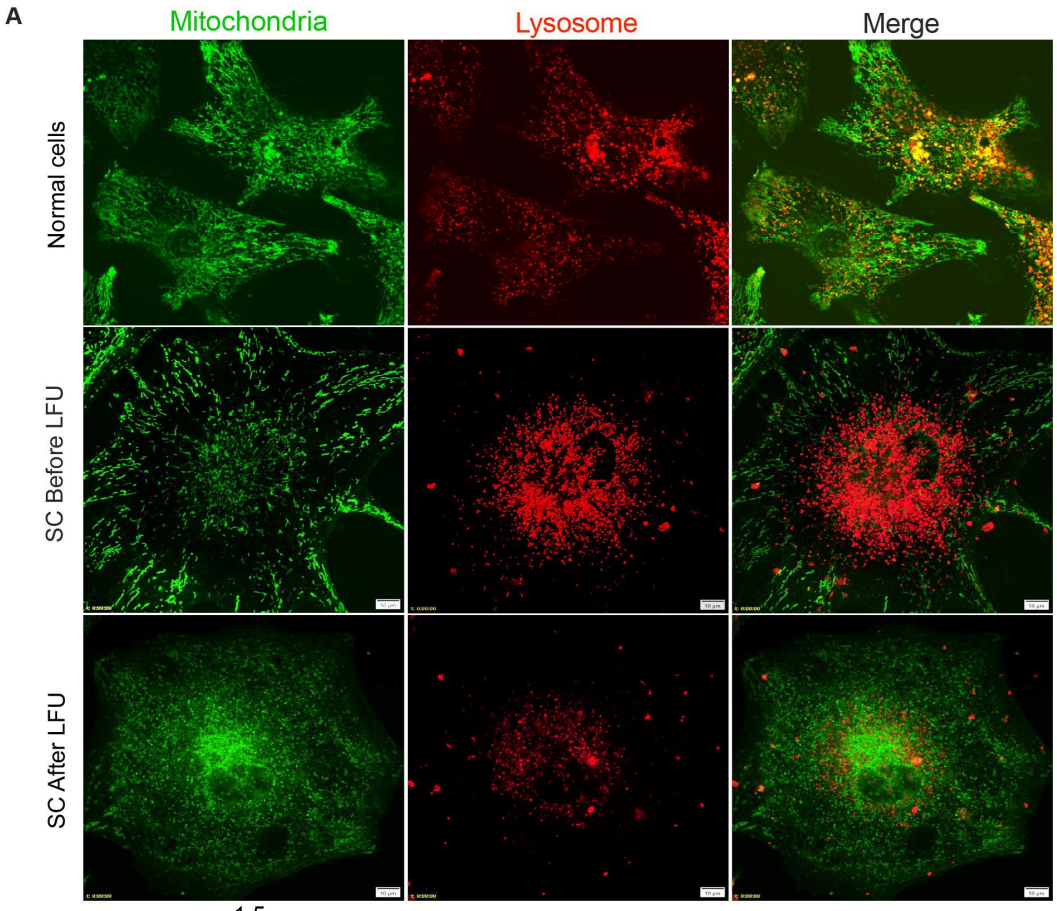

Figure 3 Low Frequency Ultrasound Decreases Mitochondrial Length and Lysosome intensity in Senescent Cells. (A) Representative immunofluorescent images of mitochondrial morphology and Lysosome fluorescence in normal, senescent and LFU-treated senescent cells stained with Mitotracker and lysosome tracker. Scale bar=10 μm. (B) Ratio of intensities of lysosomal to mitochondrial staining is decreased by ultrasound treatment of senescent cells. (C) Quantification of mitochondrial length shows decreased length after LFU. Results are shown as mean ± SD, minimum 8 cells were analyzed, n>3 experiments and significance was determined using two-tailed unpaired t-test. *** p value<0.001. (D) Diagram of a working model for the rejuvenation of senescent cells by activation of autophagy through LFU inhibition of mTORC1 activity.

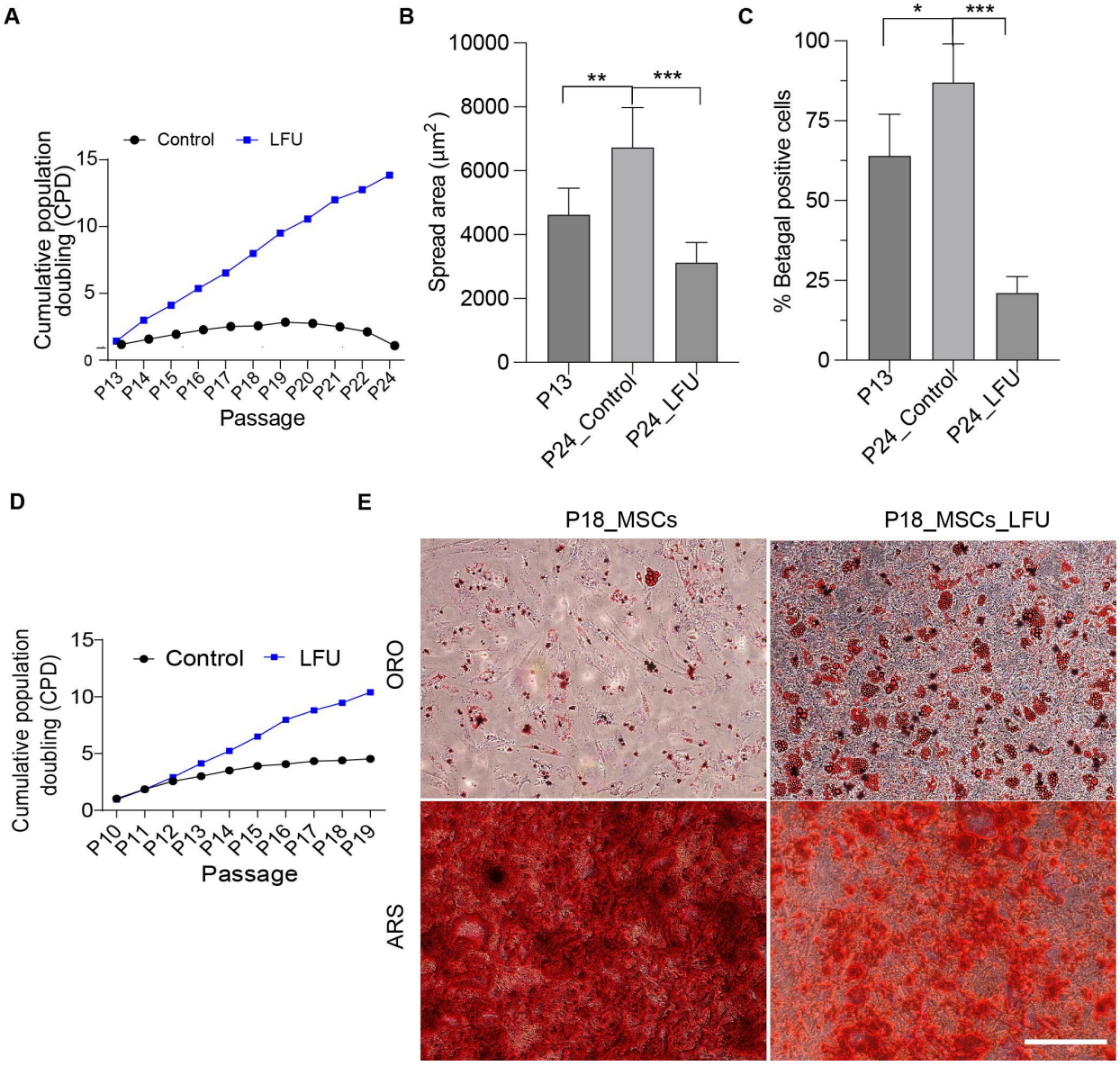

Figure 4 Ultrasound Reversal of Replicative Senescence Increases Number of Cells. (A) Growth rate calculated as cumulative population doubling (CPD) for Control HFF and LFU treated HFF cells passaged every 48 h from P13 to P24 passage with treatment every other passage (B). LFU treated cells were smaller than the p24 control and even p13 cells. (C) Number of SA-β-galactosidase positive cells decreased after LFU treatment. (D) Similarly, LFU treatment of MSCs expanded the cell number P10-P19, with treatment every other passage. (E) LFU treated MSCs showed normal differentiation to (ORO) adipocytes and (ARS) osteocytes. Alizarin red S-stained dye marked osteogenesis (ARS) and oil red o staining dye marked lipid droplets (ORO). Results are shown as mean ± SD, minimally 200 cells for spread area and 150 cells for percentage β-galactosidase analysis, n>3 experiments, and significance was determined using two tailed unpaired t-test. *** p value<0.001, ** p value<0.01, and * p value<0.05.

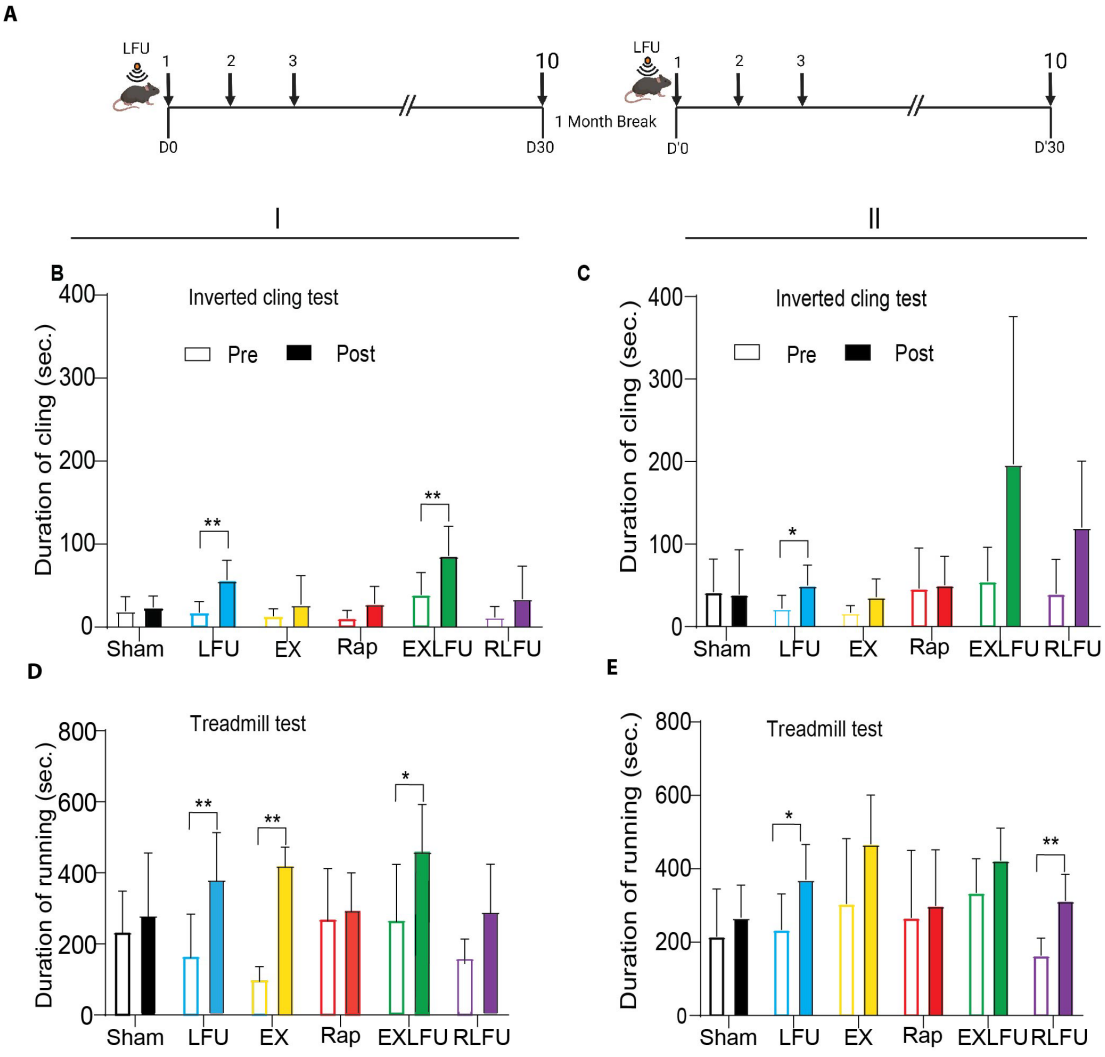

Figure 5 Effects of ultrasound treatment on performance of aged mice. (A) Schematic illustration of the treatment plan. Mice (22–24-month-old C57BL/6J strain) were LFU treated for 30 min every 3rd day or run on the treadmill 12 times for 20 min over one month (EX). There were six groups of 4 females and 4 males, Sham, LFU, EX, rapamycin (Rap), EXLFU, and rapamycin plus LFU (RLFU). After one month, they had a month bread before an additional month of treatment or exercise. (B) Graph of results of inverted cling test (see materials and methods) after the first month. and (C) after the second month of treatment. (D) Results of the treadmill test after the first month and (E) after the second month of treatment. Groups were untreated (Sham), treated with LFU, treated with exercise (EX), treated with rapamycin (RAP), treated with LFU plus exercise (EXUS),; and treated with rapamycin plus LFU (RUS). Results are plotted as mean ± S.D. Student t-test was used to determine the statistical significance. P-value greater than 0.05 is represented by ns. Statistical significance was given in p-value. *p value<0.05, **p value<0.001, and *** p value<0.0001.

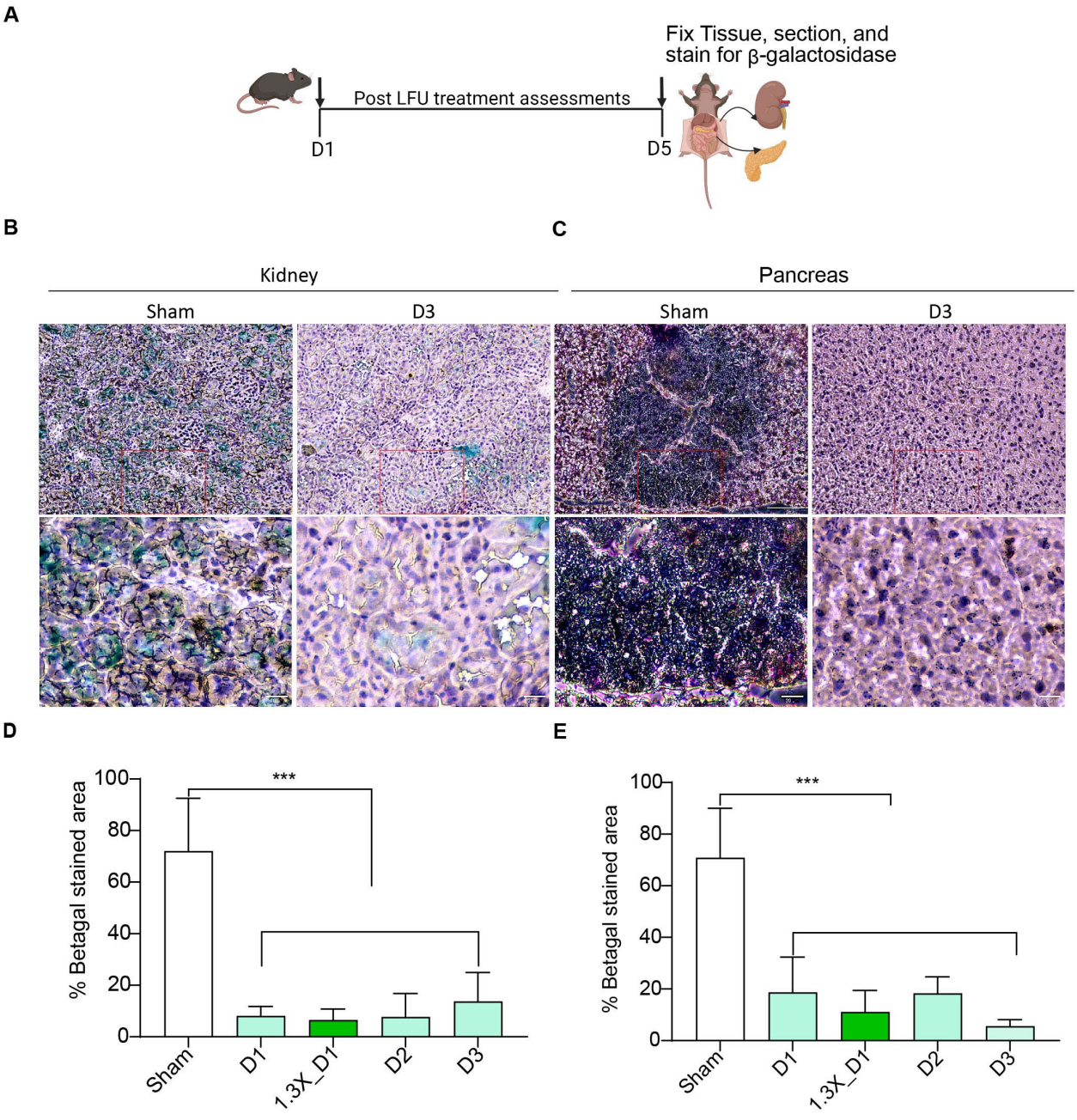

Figure 6 LFU decreases the fraction of senescent cells in kidney and pancreas.

(A) Schematic illustration of the treatment plan and tissue staining. Mice were treated 30 min every day (D1), every other day (D2) and every third day (D3) day for two weeks then two weeks break and again two-week treatment. Performance of treated mice was assessed as pre and post assay. Each study group contained five male and five female mice. After 4 weeks of treatment followed by assessment, mice were euthanized, and kidney and pancreas were collected for SA-b galactosidase staining. (B) SA-b-galactosidase-stained kidney sections of sham and LFU treated mice. (C) SA-b-galactosidase-stained pancreas sections of sham and LFU treated mice. Blue color indicates b-galactosidase activity, scale bar=150 μm and 20 μm. (D) Quantification of b-galactosidase staining of kidney sections

in sham and LFU treated mice. (E) Quantification of b-galactosidase staining of pancreas sections in sham and D3 mice. Results are plotted as mean ± S.D. Student t-test was used to determine the statistical significance. P-value greater than 0.05 is represented by ns. Statistical significance was given in p-value. *p value<0.05, **p value<0.001, and *** p value<0.0001 (n=10 mice).

Supplementary Materials

Materials and Methods

1. Cell lines and Cell Culture:

Human Foreskin Fibroblast (HFF) and Bone marrow derived mesenchymal stem cells were purchased from the ATCC. African monkey kidney derived Vero cells were obtained from the M. Garcia-Blanco lab as a gift. All these cell lines were cultured as per manufacturer's protocol. Vero cells and HFF cells were in growth medium containing Dulbecco's Modified Eagle's Medium (DMEM) 10 % fetal bovine serum (FBS; Gibco) and 1% Penicillin/ Streptomycin. Human MSCs were cultured in MSCs approved medium (ATCC) and expanded as per suppliers' protocol. Culture medium was changed in every 48 h unless otherwise stated. Cells plated at 20-40% confluency were maintained in an incubator at 37^0C and 5% CO_2. Cells were passaged in every 48-72 h using Trypsin/EDTA (Gibco). Cells were counted manually using hemocytometer and ImageJ in at least three independent replicates unless otherwise stated. Minimally 5 fields were counted from each replicate.

2. MSCs Differentiation assays

LFU treated and untreated P18 MSCs were cultured in a 12-well culture plate in growth medium for 24 h. Then, growth medium was replaced by audiogenic (Invitrogen) and osteogenic (Invitrogen) differentiation media as per the manufacturer's protocol. Adipocytes were assayed after 12 days with oil red o (Sigma Aldrich) dye solution and osteocytes were assayed using Alizarin red S dye (Sigma Aldrich) solution. Images were acquired using 10x evos RGB objective.

3. Senescence induction and quantification

Vero cells were treated with various stressors including 200 mM H_2O_2, 4 mM of sodium butyrate (SB), and 25 mM of Bleomycin Sulphate (BS), 200 nM doxorubicin and incubated for 36-48 h. After washing with PBS and then adding fresh medium, cells were incubated for 4 days to confirm the growth arrest of senescent cells. Human foreskin fibroblast (HFF) cells were serially passaged up-to p15 since replication of these cells was dramatically reduced by p15-17. We used four criteria to determine if cells were senescent; (1) Cell cycle arrest by determining the growth rate, (2) Increase in cell spread area, (3) Development of senescence associated secretory phonotype (SASP) in culture medium, and (4) b-galactosidase staining. We captured images of cells with an Evos microscope at 10 X magnification

after treatment and 48 h post treatment. To measure growth by the increase in cell number, 15 random images were captured, then the average number of cells were determined, which was divided by the area of one frame to get the cell density (cells/cm^2). Then this seeding density was multiplied by the total area of the dish or well to obtain the total number of cells after LFU treatment and after 48 h if incubation. The total number of cells at 48 h was divided by the total number of cells just after LFU treatment to determine the growth rate. If the ratio was one, there was no growth.

Senescence was detected by the b-galactosidase senescence staining kit as per manufacturer's protocol. Briefly, sub-confluent senescent cells were stained by the SA-b-galactosidase staining solution and incubated overnight at 37^{0}C. The β-galactosidase-stained cells appeared blue and were Senescent cells. The percentages of b-galactosidase positive cells were determined by counting the number of blue cells and dividing by the total number of cells. Cell spread area was determined by capturing the mages of cells with a 10X objective using an Evos microscope. Then, we used ImageJ software to calculate spread area by manually encircling the cell periphery of each cell. We used minimum 150 cells for the analysis. To determine the SASP activity, we cultured the senescent cells for 3-4 days and then supernatant was collected from each dish. This supernatant was used to culture normal cells. Development of a senescence phenotype by the normal cells in supernatant medium confirmed that senescent cells were secreting SASP.

4. LFU treatment of cells

Prior to LFU treatment, the plates containing senescent Vero cells or late passage HFF cells were wrapped with parafilm to avoid contamination and water influx into the plate. The samples were placed on the plastic mesh, which was mounted on the water tank with an ultrasound transducer. Water in the tank was degassed and heated to 35^{0}C. The distance between the sample and transducer was approximately 9-10 cm. We also ensured that there were no air-bubbles or air-water interfaces between the water and the sample. Output power of the transducer was measured at the plate location by a calibrated hydrophone. Cells were treated with pressure pulses of intermediate power and low frequency for 30 mins. Cells were treated with a 50% on-off duty cycle. After LFU treatment, cell plates were returned to the incubator for 48 h to determine the growth of senescent cells.

5. Reversal of senescence

First, we induced senescence in Vero cells using sodium butyrate, then we confirmed senescence using growth arrest and b-galactosidase staining. We treated the senescent cells using LFU of optimized parameters (power, frequency, and duty cycle). We incubated these cells for 48hr and we measured the growth and morphology of the cells before trypsinization. We named this passage P0. These cells were then trypsinzed, reseeded, and incubated for 48 hr. in the

P1 passage. This process was repeated to P3 passage. We evaluated the cells in terms of fold change in number for growth, morphology, b-galactosidase, and EDU staining to check the population of senescent cells. Senescent cells without LFU treatment were used as control cells. Typically, by passage P3, the senescent cells exhibited the phenotype of normal proliferating cells.

Passage 15-24 HFF cells were treated with LFU at the optimized frequency and power. Cell proliferation was determined by counting the number of cells at the time of seeding and 48 h post LFU treatment. LFU treated HFF cells showed higher greater growth than the untreated HFF cells. In the case of control P24 HFF cells, they were treated LFU and incubated for 96h prior to trypsinization, reseeding and incubation for 48 hours. Proliferation and morphology were measured after 48 of incubation. P24, LFU treated HFF cells became smaller in size, and they also showed dramatically greater proliferation than the untreated P24 HFF cells.

6. Soft surface preparation:

PDMS of 5 kPa elastic modulus was prepared by mixing the Sylgard 184 silicone elastomer kit containing Elastomer/curing ratio in 75:1. The combination was mixed, degassed and spin coated at 4000 rpm for 20 seconds on 27 mm ibidi glass bottom dishes. PDMS coated dishes were incubated at 65 °C overnight. Dishes were cleaned, functionalized by oxygen plasma treatment, then coated with 25 µg/ml Fibronectin (Sigma Aldrich) and kept overnight at 4 °C. Coated dishes were washed with PBS before plating the cells.

7. Microtubule analysis

Senescent cells were treated with tubulin tracker deep red (Invitrogen) as per manufacturer's protocol. Briefly, cells were incubated in tubulin tracker at 1000:1 for 30 min and medium was changed before confocal imaging with a 60x oil objective. The cells were treated with LFU and imaged again at the same confocal microscope settings. Length of myotubules was determined as described previously (Singh et al. 2021).

8. Pharmacological drug treatment

The following inhibitors were used in the study: Nocodazole (1mM), Cytochalasin D (100 nM), Blebbistatin (10 mM), Y27632 (1 mM), EX-527 (10 mM), and Rapamycin (1 mM). Senescent cells were incubated in Resvetrol (100 mM) for 24 h to activate the Sirtuin 1 activity. All inhibitors were purchased from Sigma Aldrich and prepared in DMSO and milli water as per manufacturer's protocol. Cells were incubated in inhibitors overnight after 6-8 h cells seeding. LFU treatment was performed after overnight drug addition.

9. Senescence assay

Senescence was detected by the senescence associated b-galactosidase staining (Sigma Aldrich) as manufacturer's protocol. Briefly, Senescent, non-senesncent and LFU treated cells were seeded in 27 mm ibidi glass bottom dish and incubated for 48 h. Then, these cells were fixed and stained as manufacturer's protocol. After adding staining solution into the dish, cells were incubated overnight at 37°C in absence of CO2. A minimum of 100 cells were counted manually for each condition of the analysis.

Ten–15 random images were captured for each condition for analysis of b-galactosidase positive cells that were counted manually.

10. EDU staining

Cells were incubated with 10 mM EDU reagent for 24 h. Cells were then fixed, permeabilized and blocked according to the manufacturer's protocol (Click-iT EdU Alexa Fluor 555 imaging kit, Life Technologies). Hoechst was used to stain nuclei at 5000:1 ratio. Images were captured with a 10X objective. The number of red puncta over the total number of blue nuclei gave the percentage of EDU positive cells. At least 200-300 cells were counted manually using ImageJ for each analysis.

11. Mitochondrial morphology

Ultrasound treated cells were incubated with Mitotracker (Invitrogen) in 100 mM at 37^{o}C for 30 min. Then, Images were captured in a Confocal microscope at 15 randomized fields per sample for quantification. Aspect ratio and form factors were determined using the formula Major axis/ Minor axis and Perimeter2/ (4π x surface area)[1].

12. Immunofluorescence staining

Cells were fixed with 4% paraformaldehyde for 15 minutes, permeabilized with 0.5% Triton-X for 5 min, and blocked with 3% Bovine serum albumin (BSA) for 1 hour at the room temperature and then incubated in primary antibody overnight at 4^{0}C. The following primary antibodies were used; rabbit polyclonal p21 antibody (cell signaling) (400:1), Mouse monoclonal p16 antibody (300:1) (abcam), Mouse monoclonal SIRT1 antibody (300:1) (Sigma). After washing with PBS, cells were incubated with goat anti mouse 488 (1000:1) (Sigma) and Donkey anti rabbit 555 (1000:1) (Invitrogen) for 2 h. Nuclei were stained with Hoechst at 5000:1 ratio. Images were acquired in a confocal microscope. Mito tracker green (Invitrogen) at 100 nM, Lysosome tracker deep red (Invitrogen) at 50 nM, and Tubulin tracker deep red 1000:1 were used as fluorescent probes.

13. Animals

All mice used in the study were purchased from Jackson's lab (JAX 000664 and CF7BL/6J strain) and maintained in the Animal research center (ARC) at UTMB. All animal-related procedures including housing, euthanasia, non-survival surgery, tissue collections and experimental procedures were approved by the Institutional Animal Care and Use Committee (IACUC) in the protocol number 2102013, at UTMB Galveston. Each experimental group was comprised of 22-25 month old mice with male and females. Equal numbers of mice were used in each group unless otherwise stated. Rapamycin-treated mice were fed with (1819023-201 Mod LabDiet® 5LG6 w) 143 ppm Encapsulated 3/8" Rapamycin.

14. LFU treatment of Aged mice

Aged mice (21-24 months old) were treated in a 4L glass beaker with an internal plastic cylinder of 13 cm height and 15.2 cm in diameter. A plastic mess was placed on top the cylinder that supported the mice and enabled them to rest with their four limbs and body in the water. Degassed, 32-35°C water was poured into the beaker to a level of 1 inch above the plastic mesh so that half of the bodies of the mice were in water. Once the mice were placed in the water, intermittent ultrasound of low frequency and intermediate power was applied to the mice. The reason for putting animals in water was that ultrasound was attenuated dramatically at air-water interfaces. Animals in the ultrasound groups were treated at 72-96 h intervals for one month (10 treatments). During the ultrasound treatment, we carefully observed mouse activity and their adaptation to the system. After treatment, the animals were placed in a separate cage with tissue paper to dry the animals and then they were returned to their home cage. Control mice were placed in the same water bath for 30' without ultrasonication.

15. Physical assessment of the mice

For assessment of the effect of LFU treatment on physical performance of the mice, we used 6 groups of old mice, 1. Sham, 2. LFU treatment, 3. Exercise treatment, 4. Rapamycin, 5. Exercise plus LFU, and 6. LFU plus Rapamycin. Each group contained four males and four females. In the case of the rapamycin-treated animals, the C57BL/6J mice were fed with encapsulated rapamycin and monitored daily for a month. Animals of LFU groups were treated every 72-96 h for a month. Animals in the exercise group were trained three times per week on a treadmill for 25' in each exercise training session. Prior to starting the experiment, we assessed the physical functions and health condition of the mice, identified as pre-assessment. After one month of LFU treatment and/or exercise sessions, we again assessed the physical performance and health conditions of the animals, identified as post-assessment. Physical performance

was determined by the functional assessment tests including Grip test, Rotarod, Treadmill, and Inverted Cling tests (33).

a) Rotarod: A rotarod device allowed us to quantify overall neuromuscular function: endurance, balance, and coordination. The whole procedure involves 2 training days and 1 day for testing. During the training days, the animals were acclimated to the device. On the test day, three trials were conducted per session with resting periods of 10 min in between trials. The outcome measurement was the average duration of the animal on the rod.

b) Inverted Cling: This grip test was useful to quantify muscle strength and endurance by measuring how long the mouse held onto the grid while inverted. Each animal was tested 2 times with a resting break of 10 min between trials. A minimum holding time of 10 seconds was required for test validation to exclude a slip. Three trials were conducted with a gap of 10 mins between trials.

c) Treadmill: The mice were tested for the maximum power output/maximum gait speed and endurance (to exhaustion) by running on a treadmill. The measurement was the duration of the running. During the training session, the mice were familiarized with the device, first running at a constant speed, later increasing the speed progressively one unit in every 20 seconds. The mice were allowed to rest 10 min between trials. Three electric shocks of 0.4 mA ended the trial and animals were given three trials. During each trial, the speed was increased one unit in every 20 seconds, and each mouse was allowed to run as long as they could before getting three shocks.

d) Exercise training sessions: Animals of Exercise and Exercise + LFU groups were exercised on a treadmill for 25 min at three times in a week for one month. Every exercise session was preceded by 10 min warm up at 6 cm/s, followed by 10 min training at 8 cm/s, and 5 min cool down at 6 cm/s. Training was progressive starting at 8 cm/s in the first week and increasing to 11 cm/s in week 4. The mice were encouraged to run on treadmill with a light electric shock when they stopped running. There were 12 exercise training sessions and 10 LFU treatments in the one month experimental period.

16. Immunohistochemistry

Kidney and pancreas were collected after completion of post physical assessment under deep anesthesia. Both the organs were flash frozen in isopentane -liquid nitrogen. Organs were sectioned in a -20°C cryostat and stored at -20°C. Kidney and pancreas sections of 6-8 um thickness were fixed and stained with SA b-galactosidase as described in the manufacturer's protocol. Sectioned samples were incubated at 37°C in a CO2-free incubator.

Sections were stained with hematoxylin and eosin y for cytoplasmic and nuclear staining per standard protocol. Images were captured at 20X in the RGB channel of EVOS microscope. The fraction of b-galactosidase stained tissue was determined using ImageJ.

17. Immunofluorescent detection of p21 and p16 in Kidney and Pancreas

Pancreas and Kidney sections were immunoassayed by treating with 4 % paraformaldehyde for 15 minutes, permeabilizing with 0.5% Triton X-100 in PBS for 2 min at 25°C, blocking with 10% Bovine serum albumin for 1 hour at 25°C, and incubating with rabbit anti-p21 antibody (Abcam, ab188224) I and mouse p16 antibody (Cell signaling) overnight at 4°C. Fluorescent secondary antibodies [Invitrogen, goat anti- mouse 488 (800:1) and donkey anti-rabbit 555 (800:1) were added, and the samples were incubated at 4°C for 4 hr in a humidified chamber followed by washing with PBS. Images were acquired with an Olympus light microscope using 60x oil objective. A minimum of five unique fields of view were analyzed per sample of pancreatic and kidney tissue obtained from four mice per group.

18. Statistical analysis

All results are shown as mean ± s. d. and paired t-test, two tails used for two groups. GraphPad Prism 8.4.3. was used for making graph and statistical analyses. * P values<0.05, ** p values< 0.002, *** p values <0.001, and non-significant (ns) p-value >0.05 were used, shown in figures.

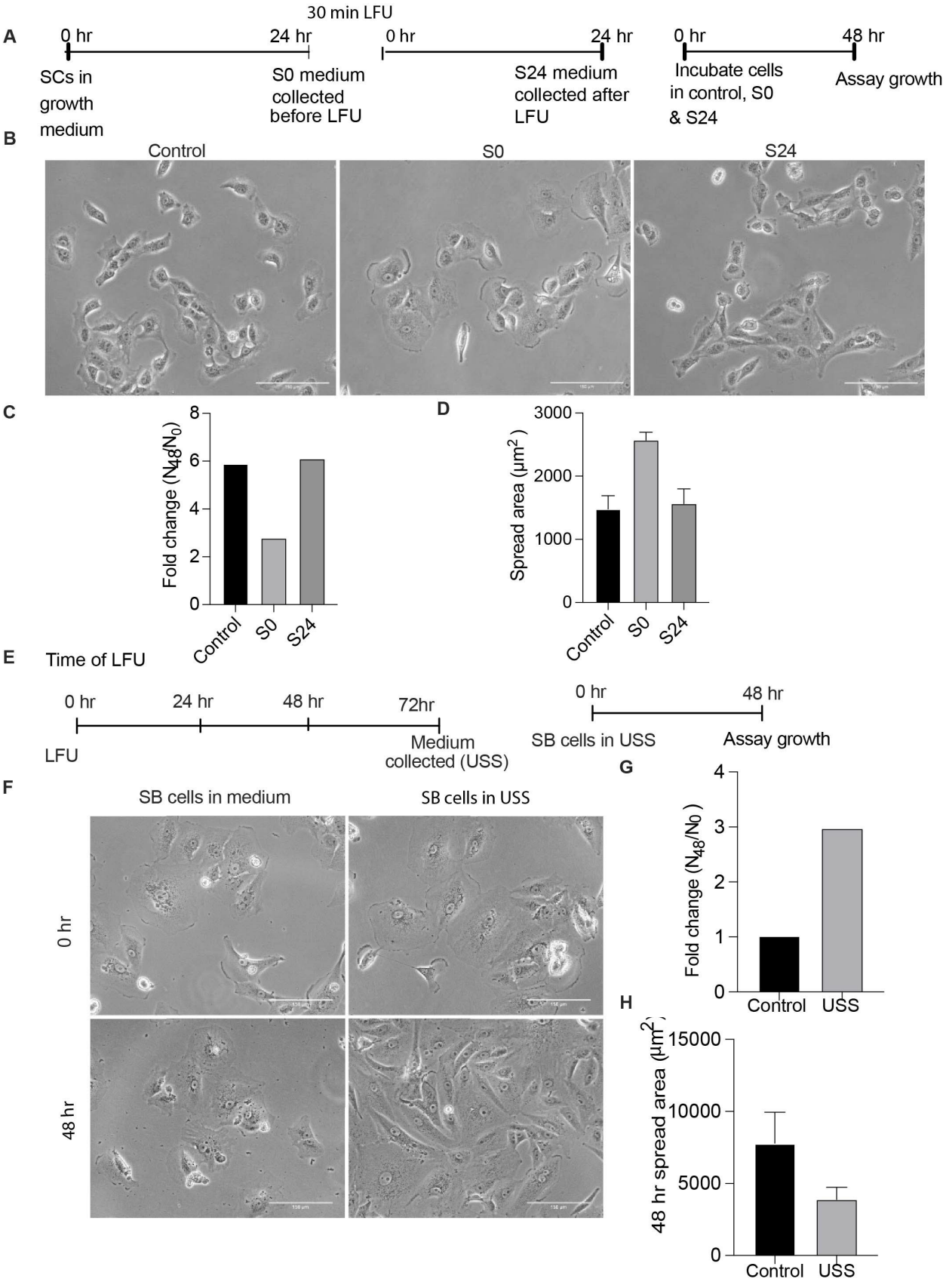

Figure S1 SASP inhibits Control, but USS increases senescent cell growth. (A) Schematic illustration of the experiment. SCs were cultured in growth medium for 24 hr then they were treated with low frequency ultrasound (LFU) for 30 min. Supernatant was collected after the LFU treatment (S0) and again supernatant was collected after 24 h (S24). To check the effect of LFU treatment, supernatants S0 and S24 were used to check the growth of non-senescent HFF cells. (B) Representative brightfield images of control cells after 48 hours of incubation in normal growth medium, S0, and S24. Quantification of control cell numbers shows (C) and cell areas (D) after 48 in control, S0 or S24 supernatants. (E) Timeline and strategy of schematic of LFU treatment of normal proliferating cells. Schematic showing that control cells were treated with US four times in the same media and the supernatant was collected (USS) for incubation of senescent cells for 48 h. (F) Brightfield images shows change in morphology of SCs in supernatant collected from LFU treated control cells and after 48 h in response to USS. Senescent cells in normal growth medium were the controls. (G) Graph shows growth of SCs in USS increased and (H) decreased spread area of senescent cells. Graphs were plotted by mean ± SD. Minimum 200 cells were analyzed for graph (C) and (H). Scale bar= 300 µm.

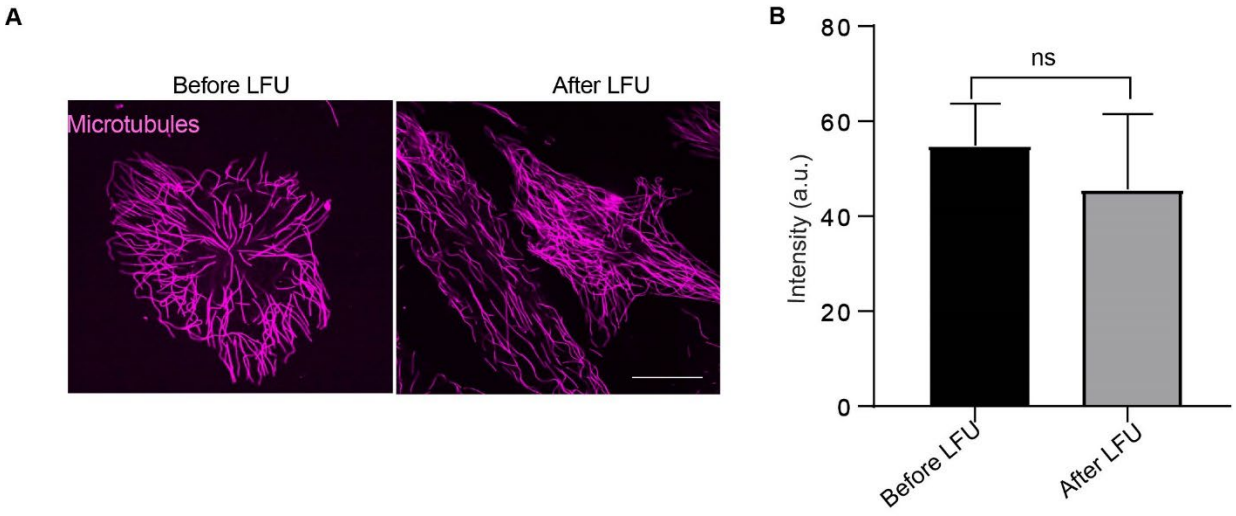

Figure S2 Low frequency ultrasound has no effect on microtubules. (A) Representative fluorescence images of microtubules in senescent cells. Scale bar = 10 µm. (B) Intensity of microtubule was quantified from (A). Results are plotted as mean ± S.D. Student t-test was used to determine the statistical significance. P-value greater than 0.05 is represented by ns. Statistical significance was given in p-value. *p value<0.05, **p value<0.001, and *** p value<0.0001.

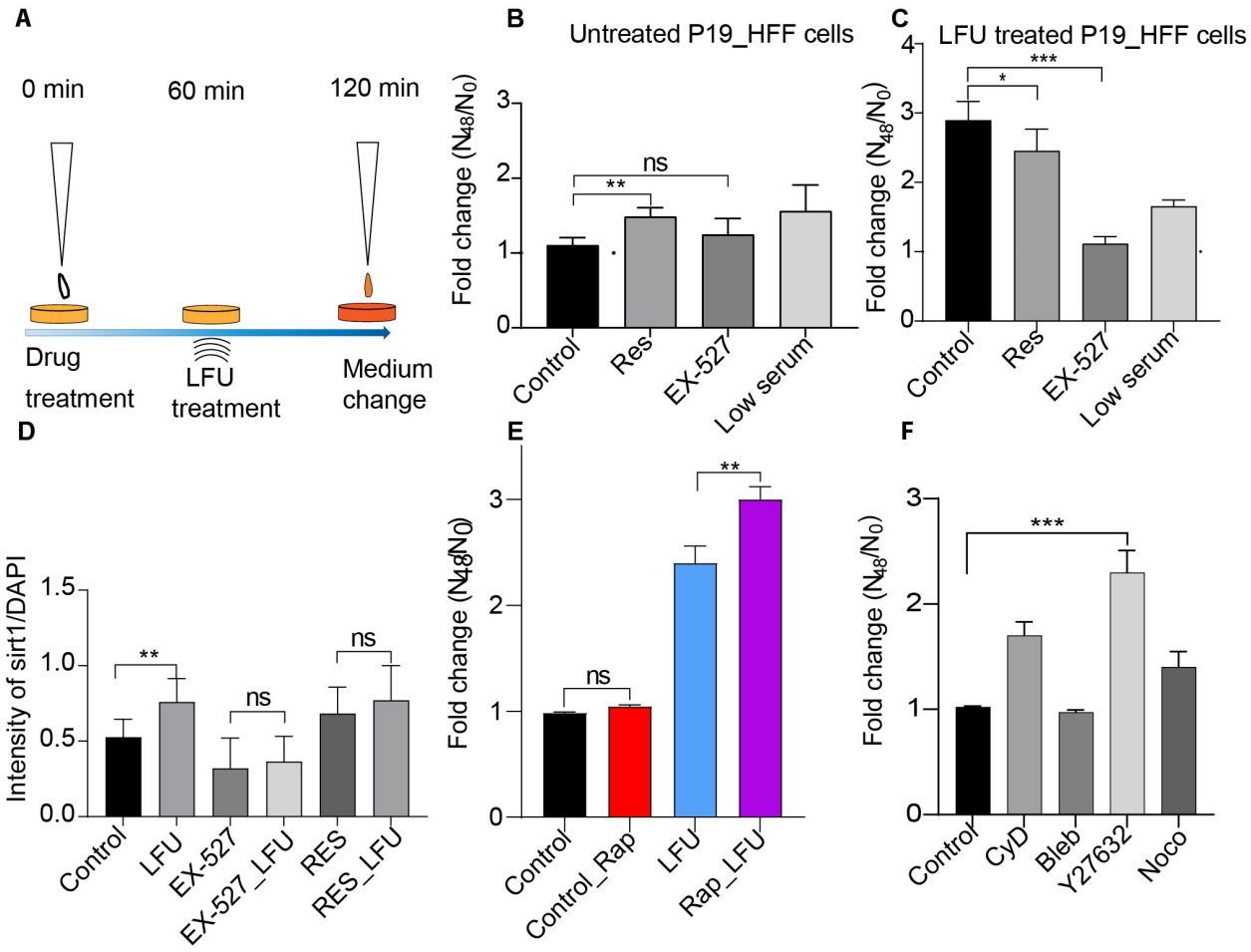

Figure S3 Ultrasound has no effect on cells after sirtuin1 inhibition. (A) Schematic of Resveratrol and EX-527 treatment, followed by Ultrasound treatment and medium change. (B) Growth of untreated control HFF cells in presence of drug and (C) growth of LFU treated HFF cells. (D. quantification of sirt1 expression by intensity ratio of sirt1 and DAPI. (E) Growth rate significantly increased in rapamycin and LFU treated SCs compared to with and without rapamycin. (F) Growth of SCs in presence of cytoskeleton inhibitors including Cytochalasin D, Blebbistatin, Y27632, and Nocodazole. Results are shown as mean ± SD. ** p value <0.02 and 'ns' p value >0.05.

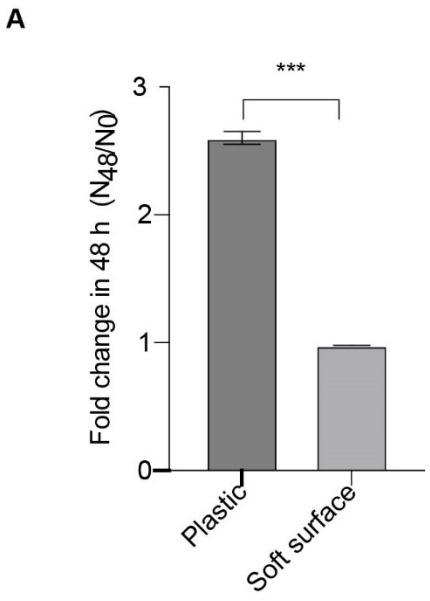

Figure S4 Growth of Rejuvenated cells on soft or rigid surfaces. (A) Rejuvenated cells grow on stiff substrate whereas their growth ceased on soft surface. Results are shown as mean ± SD. ** p value <0.002.

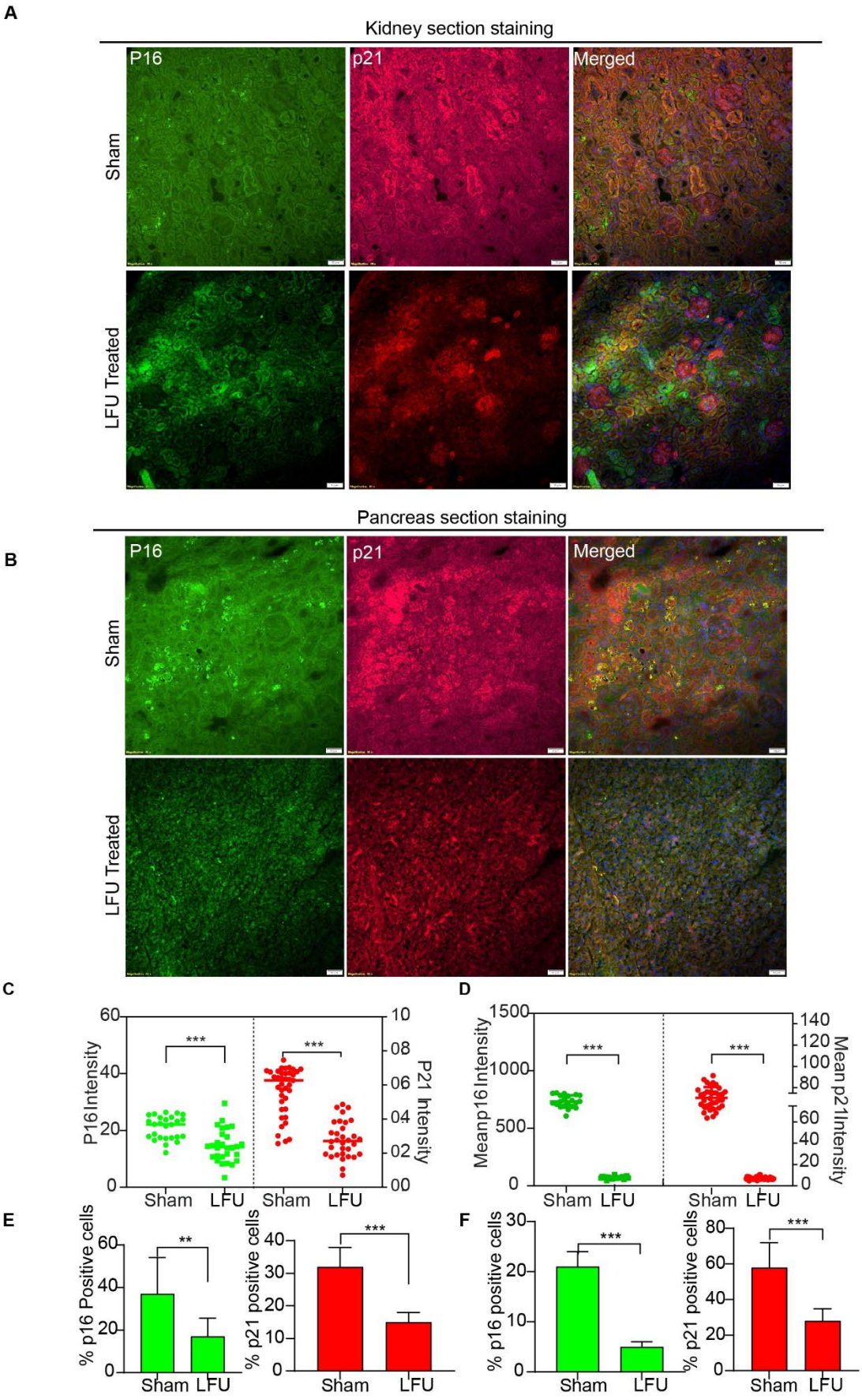

Figure S5 Senescence Effect of LFU treatment of kidney and pancreas on p16 and p21 senescence markers. (A) Representative fluorescence images of p16 and p21 immunostaining of kidney section. Scale bar= 10 μm. (B) Representative fluorescence images of p16 and p21 immunostaining of pancreas section. Scale bar= 10 μm. (C) Quantification of p16 and p21 stained kidney section, (D) Pancreases. (E) Quantification of percentage p16 and p21 positive cells in kidney section and (F) Pancreas sections.. Results are shown as mean ± SD. *p value<0.05, **p value<0.001, and *** p value<0.0001.

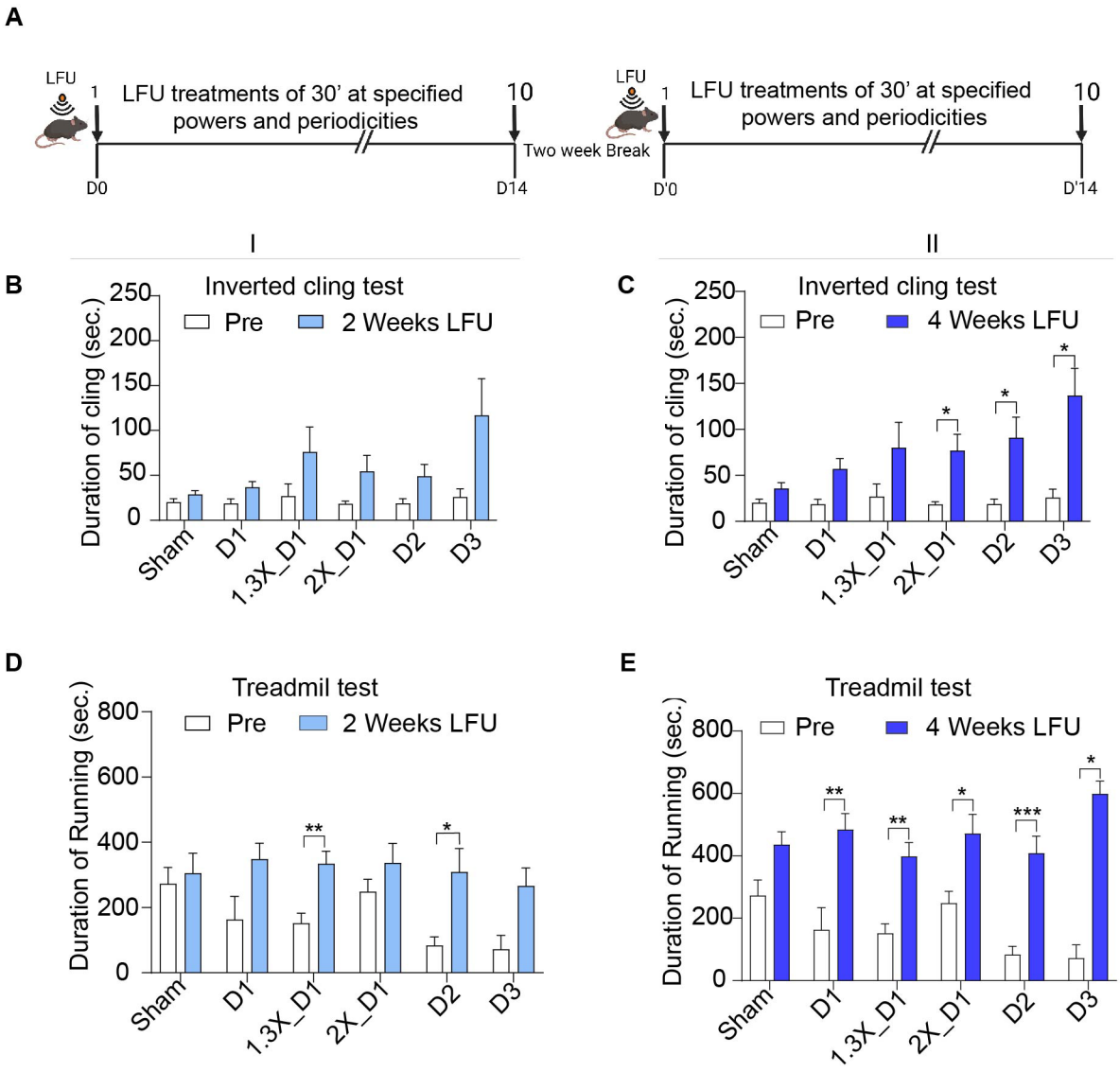

Figure S6 Effects of ultrasound treatment on performance of aged mice. (A) Schematic illustration of the treatment plan. Mice were treated 30 min at 1X power every day (D1), every other day (D2) and every third day (D3), 1.3x power every day (1.3X_D1) or 2X power every day (2X_D1) for two weeks then two weeks break and again two-week treatment. Performance of treated mice was assessed as pre and post assay. 20-24 months old mice (C57BL/6J strain) were treated every 72 hrs and exercise training sessions were conducted 3 times per week. Each study group contained five male and five female mice. (B) Results of inverted cling test for the first two weeks LFU treatment. and (C) Inverted cling test data of four weeks treatment after 2 weeks break. (D) Results of the treadmill test for the first two weeks LFU treatment (see Materials and Methods mouse protocols). (E) Results of the treadmill test (see Materials and Methods mouse protocols) data of four weeks treatment after two weeks break. Results are plotted as mean ± SEM. Student t-test was used to determine the statistical significance. Statistical significance was given in p-value. *p value<0.05, **p value<0.001, and *** p value<0.0001.